

# Design and Analysis of Ultra-High-Speed Near-Ballistic Uni-Traveling-Carrier Photodiodes Under a 50- $\Omega$ Load for High-Power Performance

Jin-Wei Shi, Feng-Ming Kuo, and John E. Bowers

**Abstract**—We demonstrate a near-ballistic uni-traveling-carrier photodiode (NBUTC-PD) with a scaled-down epi-layer structure designed for high-power performance in the sub-THz frequency regime. Compared with UTC-PDs, NBUTC-PDs offer a higher optimum bias voltage for the near-ballistic transport of electrons, which leads to improvement in the output power performance. Furthermore, a small load resistance ( $<50\ \Omega$ ), which would sacrifice the output power for minimizing the output ac voltage swing on dc bias point, is not necessary. By scaling down the collector layer thickness and active area of the NBUTC-PDs, we achieve a large optical-to-electrical bandwidth (250 GHz) and a high saturation current (17 mA), which is close to the theoretical maximum, under a 50- $\Omega$  load and -2-V bias.

**Index Terms**—High-power photodiode, photodiodes, photonic transmitter.

## I. INTRODUCTION

MILLIMETER wave (MMW)-over-fiber systems are considered to be one of the most suitable candidates to meet the demand of future ultra-broadband wireless access networks [1]. The key component of such systems is the photonic transmitter (PT), which is composed of a high-power/speed photodiode (PD) and antenna [1]. By using advanced traveling-wave structures [2] or uni-traveling carrier photodiodes (UTC-PDs) [3,4], PDs with both ultra-wide optical-to-electrical (O-E) bandwidth and high-saturation current have been demonstrated [2-5]. In order to attain a UTC-PD with a O-E bandwidth of around 300 GHz, the thicknesses of the collector and absorption layer need to be scaled down to  $\sim 200$  and  $< 100$  nm [3,4], respectively. This is necessary to effectively shorten the internal transient time, usually accompanied by a small device active area ( $< 10\ \mu\text{m}^2$ ) and a small load resistance ( $< 50\ \Omega$ ) for sustaining a high RC-limited bandwidth [3,4]. However, this approach could cause serious

Manuscript received September 13, 2011; revised November 30, 2011; accepted December 7, 2011. Date of publication December 14, 2011; date of current version March 7, 2012. This work was supported in part by the National Science Council (NSC) of Taiwan under Grant NSC-100-2918-I-008-004 and in part by DARPA MTO PICO Project.

J.-W. Shi and F.-M. Kuo were with the Department of Electrical Engineering, National Central University, Taoyuan 320, Taiwan. They are now with the Department of Electrical and Computer Engineering, University of California, Santa Barbara, CA 93106 USA (e-mail: jwshi@ee.ncu.edu.tw; 975201125@cc.ncu.edu.tw).

J. E. Bowers is with the Department of Electrical and Computer Engineering, University of California, Santa Barbara, CA 93106 USA (e-mail: bowers@ece.ucsb.edu).

Color versions of one or more of the figures in this letter are available online at <http://ieeexplore.ieee.org>.

Digital Object Identifier 10.1109/LPT.2011.2179795

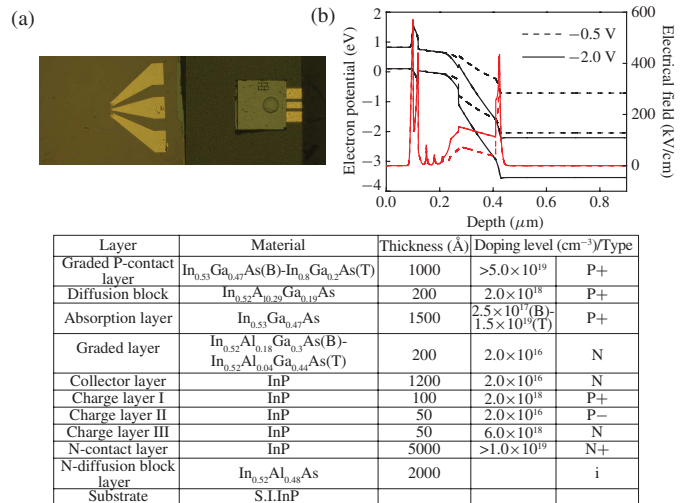


Fig. 1. (a) Top-view (before and after flip-chip bonding) and (b) simulated 1-D electric field of our structure under -0.5- and -2-V bias voltages. The inserted table shows our epi-layer structure. B: bottom; T: top.

degradation of the output power and external responsivity ( $< 0.03\ \text{A/W}$  [3,4]). Furthermore, the optimized transient time limited bandwidth ( $\sim 300$  GHz) with near-ballistic transport phenomenon of electron and maximum THz generation power only occurs near zero bias operation (-0.7 V) [3,4]. Due to its higher optimum bias voltage [1,5], the use of a near-ballistic uni-traveling carrier photodiode (NBUTC-PD) under a standard 50  $\Omega$  load is one possible solution to further improve the power performance of UTC-PD in sub-THz regime. In this study, we analyze in detail the dynamic behavior of a miniaturized NBUTC-PD ( $16\ \mu\text{m}^2$ ) with a 155 nm collector layer thickness [6]. Ultra-wide 3-dB O-E bandwidths (250 GHz), a reasonable responsivity (0.08 A/W), and a 17 mA saturation current, under a 50  $\Omega$  load is demonstrated. The device modeling results show that such a wide O-E bandwidth is RC-limited with an transient time limited bandwidth far over 300 GHz even under a moderate reverse bias (-2V).

## II. DEVICE STRUCTURE AND MEASUREMENT SETUP

Figure 1(a) shows the top view of the demonstrated device. The inserted Table shows the detail epi-structure grown on a semi-insulating (S.I.) InP substrate. The thickness of the p-type linear graded doped  $\text{In}_{0.53}\text{Ga}_{0.47}\text{As}$  based photo-absorption layer (P) is 150 nm, which is thicker than that reported for UTC-PDs (150 vs.  $< 100$  nm) with a sub-THz O-E bandwidth

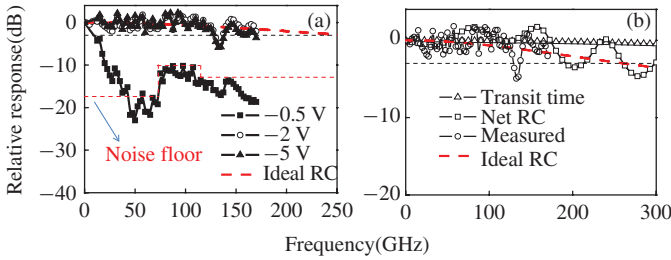


Fig. 2. (a) Bias dependent O-E frequency responses measured under a fixed photocurrent (4 mA) and (b) O-E frequency responses measured under  $-2\text{ V}$  (open circles), extracted RC-limited (open squares), and the extracted transient-time frequency responses (open triangles). The extracted ideal RC-limited (pad de-embedding) frequency response (dashed lines) are shown for reference.

[3,4]. A 120 nm thick InP layer is utilized as the collector layer (C). As can be seen in the inserted Table in Figure 1, we adopt 20 nm thick graded doping profiles on both the p- and n-sides of our InP based charge layer in order to minimize the peak electric field at the interface of the p-n junction and avoid the problem of breakdown. Figure 1 (b) shows the simulated 1-dimensional electric-field distribution for our device structure under  $-0.5$  and  $-2\text{ V}$  reverse bias voltages. We can clearly see that when the reverse bias reaches  $-2\text{ V}$ , the collector layer can be fully depleted and the peak E-field in the charge layer is around  $450\text{ kV/cm}$ , which is less than the breakdown field of the InP layer ( $\sim 550\text{kV/cm}$ ). The total thickness of the depleted layer under  $-2\text{ V}$  is thus around 200 nm, as shown in Figure 1 (b). As shown in Figure 1 (a), the fabricated device with an active area of around  $16\text{ }\mu\text{m}^2$  is integrated with a co-planar waveguide (CPW) pad and flip-chip bonded to an AlN substrate, for a  $50\text{ }\Omega$  load and good heat sinking during measurement [5]. The load resistance is around 2 to 4 times larger than that of ultra-high speed PDs with  $> 100\text{ GHz}$  O-E bandwidth performance [2-4], which improves the high-power performance of our device.

### III. MEASUREMENT RESULTS AND DEVICE MODELING

The measured responsivity of our device with a  $16\text{ }\mu\text{m}^2$  active area is around  $0.08\text{ A/W}$ , higher than that reported for UTC-PDs ( $0.08$  vs.  $0.03\text{ A/W}$ ) having a smaller O-E bandwidth than that of our device ( $\sim 170$  [4] vs.  $250\text{ GHz}$ ). The dynamic performance is measured with a heterodyne beating system. A power meter with three different sensor heads is used for the range from dc to  $110\text{GHz}$ . When the measurement frequency is greater than  $110\text{ GHz}$ , a thermal MMW power meter (PM4, VDI-Erickson) is used. The maximum measurement bandwidth for our system is limited by our WR-6 waveguide based MMW probe at  $170\text{ GHz}$ . Figure 2 (a) shows the measured bias dependent optical-to-electrical (O-E) frequency responses from near dc (direct current) to  $170\text{ GHz}$  under a fixed photocurrent ( $4\text{mA}$ ). As can be seen, bandwidth due to the enhancement of electron drift-velocity under  $-2\text{ V}$  bias, when the measurement frequency increases to  $170\text{ GHz}$ , there is only a  $\sim 1.5\text{ dB}$  drop in the response. Although there is a dip in the O-E response at  $135\text{ GHz}$ , which is caused by the integrated CPW pad, this should not be an issue. It can be replaced by an impedance matching circuit to drain the

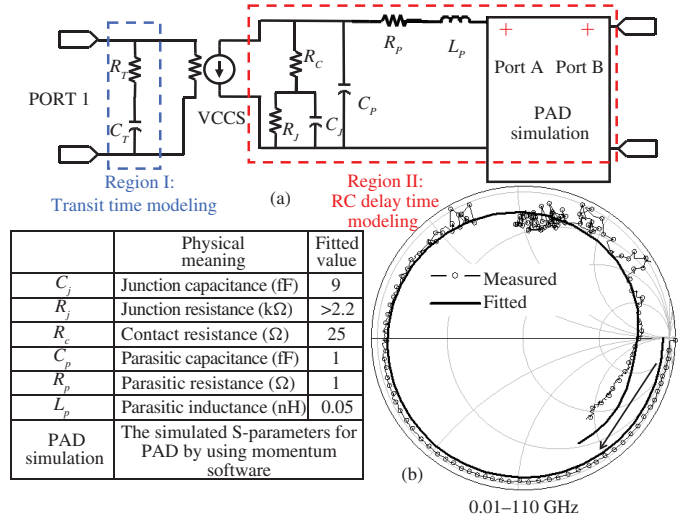


Fig. 3. (a) Equivalent-circuit-model used. The inserted table shows the extracted values of the components. (b) Measured (open circles) and fitted (continuous line)  $S_{11}$  parameters from near dc to  $110\text{ GHz}$  under a fixed dc bias ( $-2\text{ V}$ ). The arrow heads indicate the increase in the sweeping frequency.

maximum available power in the desired operating frequency at the sub-THz regime [4]. In order to estimate the 3-dB O-E bandwidth and investigate whether it is the carrier transit time or RC (resistance-capacitance)-bandwidth limitation that dominates this device, we adopt two-port equivalent-circuit-models, which include the two bandwidth-limiting factors (i.e., carrier transit time ( $f_t$ ) and RC delay time ( $f_{RC}$ )) [5], as shown in Figure 3 (a). The values used in fitting process are shown in the Table inserted into Figure 3 (a). Figure 3 (b) shows the measured and simulated frequency responses for the  $S_{11}$  reflection coefficient parameter under a  $-2\text{ V}$  bias; see the Smith chart. Clearly, the simulated and measured results match very well, from  $10\text{ MHz}$  to  $110\text{ GHz}$ . As can be seen in Figure 2 (b), there are some ripples on the extracted RC-limited frequency response (open squares), which originate from the integrated CPW pad. By de-embedding this pad in our equivalent-circuit model during simulation, we can get the ideal RC-limited frequency response (red dashed line) with a 3-dB bandwidth at around  $250\text{ GHz}$ . We can clearly see that these two extracted RC-limited frequency responses are very close to the measured net O-E frequency response, as shown in Figure 2 (b). This indicates that the internal electron transit time of the device is not the dominant bandwidth limiting factor. The extracted transient-time limited frequency response as shown in Figure 2(b) shows a negligible roll-off in our interesting frequency regime (dc- $300\text{ GHz}$ ) and the corresponding 3-dB transient-time bandwidth is much higher than that of state-of-the-art UTC-PDs ( $< 300\text{ GHz}$ ) [3] under a higher bias voltage ( $-2$  vs.  $-0.75$ ). This implies a much higher available power from our NBUTC-PD in sub-THz regime [4] due to the fact that only the internal transient time plays the key role, which limits the maximum output power [4]. Figure 4 (a) represents the photo-generated MMW power measured at  $170\text{ GHz}$  under three different bias voltages. The measured trace at  $110\text{ GHz}$  for an NBUTC-PD (Device B) which has a thicker collector layer ( $\sim 500$  vs.  $\sim 200\text{ nm}$ ) and a larger active

area ( $\sim 28$  vs.  $16 \mu\text{m}^2$ ) under a  $25 \Omega$  load is also shown here for reference [5]. Both devices have a close RC-limited bandwidth ( $\sim 300$  GHz) [5]. The ideal relation between the MMW power of a 100% modulated large-signal and the average current for a  $50$  (straight line) and  $25$  (dash line)  $\Omega$  equivalent load is also plotted for reference. As can be seen, compared with device B [5], device A can have a higher saturation current (17 vs. 12 mA) under a lower optimum reverse bias ( $-2$  vs.  $-3$ V). Based on these measurement results, we can conclude that for the same desired sub-THz RC-limited bandwidth, a scaled-down NBUTC-PD structure (area and thickness) offers a higher saturation power and a shorter transient time, which plays an important role for sub-THz power generation, as discussed. The theoretical maximum output current density can be expressed by following two equations (1 and 2) [7]. In equation 1,  $V_{\text{eff}}$  is the minimum reverse bias voltage during operation,  $J_{\text{max}}$  is the maximum output photocurrent density,  $A$  is the active area,  $V_{\text{bias}}$  and  $V_{\text{bi}}$  are the external bias and built-in potential, respectively, and  $R$  is the load resistance ( $50 \Omega$ ).

$$V_{\text{eff}} = (V_{\text{bias}} + V_{\text{bi}}) - J_{\text{max}} \times A \times R \times F \quad (1)$$

$$\kappa V_{\text{eff}} - E_c \times D_{\text{dep}} = J_{\text{max}} \left( \frac{D_{\text{dep}}^2}{\varepsilon V_e} \right) \quad (2)$$

The factor “F” in this equation represents the influence of the RC induced high-frequency roll-off on the ac voltage swing. As shown in Figure 2 (a), the RC roll-off is around 1.5 dB at 170 GHz, which corresponds to an F value of 0.84. Equation 2 represents the influence of the space-charge induced voltage on the dynamic performance of the device, where  $E_c$  is the critical field ( $10 \text{ kV/cm}$ ) for sustaining electrons with an overshoot drift-velocity ( $V_e$ ) in InP layer [8,9],  $\varepsilon$  is the dielectric constant of InP,  $D_{\text{dep}}$  is the depletion layer thickness, which is around 200 nm under a bias of  $-2\text{V}$ , and  $\kappa$  is a parameter, which represents the non-uniform potential distribution in the collector and charge layers. Based on the E-field simulation results shown in Figure 1 (b), its value is around 0.78 under  $-2\text{V}$  bias. Here, we assume that  $V_e$  has a reasonable value of  $3 \times 10^7 \text{ cm/sec}$ , which is slightly lower than the reported nonequilibrium drift-velocity of electron ( $\sim 4 \times 10^7 \text{ cm/sec}$ ). This is due to the non-negligible device-heating effect under maximum current ( $J_{\text{max}}$ ) operation [8]. The above two equations suggest that the increase in  $V_{\text{bias}}$  would result in an improvement in  $J_{\text{max}}$ . [7]. However, this is in conflict with the UTC-PD measurement results, which usually exhibit an optimum bias voltage for maximizing sub-THz output power [3,4]. This is because we have neglected the influence of electron inter-valley scattering [3,4,9] and device-heating effects [8] on  $V_e$  in the above two equations. These would become more pronounced with the increase of bias voltage on a miniaturized sub-THz PD with a transient-time limited bandwidth [3,4] and high heat-density. Nevertheless, we can still use these two equations to estimate  $J_{\text{max}}$  of PDs under their optimum bias, where these two phenomena are minor issues [7]. Furthermore, one can expect a higher  $J_{\text{max}}$  from NBUTC-PD than that of UTC-PD due to its higher value of the optimum

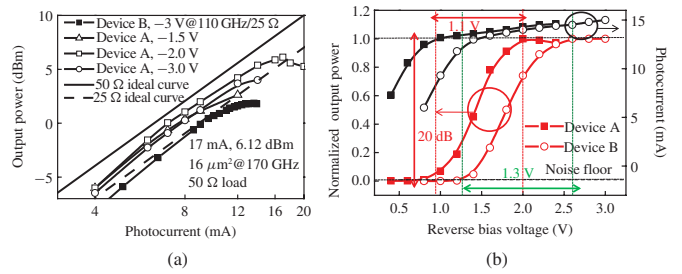


Fig. 4. (a) Measured photo-generated MMW power versus photocurrent from our device under different reverse bias voltages. (b) Transfer curve of normalized MMW power and photocurrent at 170 GHz versus reverse dc bias.

$V_{\text{bias}}$  ( $-2$  vs.  $-0.75\text{V}$ ). For our case, the calculated  $J_{\text{max}}$  is  $110 \text{ kA/cm}^2$ , which is close to our measurement results (17mA;  $106 \text{ kA/cm}^2$ ). The high bias-modulation efficiency is another key issue in PDs for wireless communication [1].

Figure 4 (b) shows the photo-generated MMW power versus bias voltage for device A and B. As can be seen, for a 20 dB power variation, the required driving-voltage of device A is smaller than that of the device B (1.1 vs. 1.3 V), which implies a higher extinction ratio of eye-patterns during wireless data transmission under the same RF driving-voltage.

#### IV. CONCLUSION

By scaling down thickness and area of a NBUTC-PD for the sub-THz bandwidth, its saturation current and transient-time bandwidth can be further improved under a lower optimum bias. Furthermore, according to dynamic analysis, NBUTC-PD has a superior output power to the UTC-PD, due to its higher optimum bias for electron near-ballistic transport.

#### REFERENCES

- [1] J.-W. Shi, C.-B. Huang, and C.-L. Pan, “Millimeter-wave photonic wireless links for very-high data rate communication,” *NPG Asia Mater.*, vol. 3, no. 2, pp. 41–48, Apr. 2011.
- [2] A. Beling, H.-G. Bach, G. G. Mekonnen, R. Kunkel, and D. Schmidt, “High-speed miniaturized photodiode and parallel-fed traveling-wave photodetectors based on InP,” *IEEE J. Quantum Electron.*, vol. 13, no. 1, pp. 15–21, Jan./Feb. 2007.
- [3] H. Ito, T. Furuta, S. Kodama, N. Watanabe, and T. Ishibashi, “InP/InGaAs uni-travelling-carrier photodiode with 310 GHz bandwidth,” *Electron. Lett.*, vol. 36, no. 21, pp. 1809–1810, Oct. 2000.
- [4] H. Ito, T. Furuta, F. Nakajima, K. Yoshino, and T. Ishibashi, “Photonic generation of continuous THz wave using uni-traveling-carrier photodiode,” *J. Lightw. Technol.*, vol. 23, no. 12, pp. 4016–4021, Dec. 2005.
- [5] J.-W. Shi, *et al.*, “Extremely high saturation current-bandwidth product performance of a near-ballistic uni-traveling-carrier photodiode with a flip-chip bonding structure,” *IEEE J. Quantum Electron.*, vol. 46, no. 1, pp. 80–86, Jan. 2010.
- [6] J.-W. Shi, F.-M. Kuo, M. Rodwell, and J. E. Bowers, “Ultrahigh speed (270 GHz) near-ballistic uni-traveling-carrier photodiode with very-high saturation current (17 mA) under a 50% load,” in *Proc. IEEE Photon. Soc. Meet. 2011*, Arlington, VA, Oct., pp. 21–22, paper MC-2.
- [7] N. Li, *et al.*, “High-saturation-current charge-compensated InGaAs-InP uni-traveling-carrier photodiode,” *IEEE Photon. Technol. Lett.*, vol. 16, no. 3, pp. 864–866, Mar. 2004.
- [8] W. Fawcett and G. Hill, “Temperature dependence of the velocity/field characteristic of electrons in InP,” *Electron. Lett.*, vol. 11, no. 4, pp. 80–81, Feb. 1975.